J Neurophysiol 112: 1179–1191, 2014.
First published June 11, 2014; doi:10.1152/jn.00040.2014.

Basal forebrain dynamics during a tactile discrimination task

Eric Thomson,[1,5] Jason Lou,[1] Kathryn Sylvester,[1] Annie McDonough,[1] Stefani Tica,[1] and Miguel A. Nicolelis[1,2,3,4,5]

[1]*Department of Neurobiology, Duke University, Durham, North Carolina;* [2]*Department of Biomedical Engineering, Duke University, Durham, North Carolina;* [3]*Department of Psychology and Neuroscience, Duke University, Durham, North Carolina;* [4]*Center for Neuroengineering, Duke University, Durham, North Carolina; and* [5]*Edmond and Lily Safra International Institute for Neuroscience of Natal, Natal, Brazil*

Submitted 13 January 2014; accepted in final form 9 June 2014

Thomson E, Lou J, Sylvester K, McDonough A, Tica S, Nicolelis MA. Basal forebrain dynamics during a tactile discrimination task. *J Neurophysiol* 112: 1179–1191, 2014. First published June 11, 2014; doi:10.1152/jn.00040.2014.—The nucleus basalis (NB) is a cholinergic neuromodulatory structure that projects liberally to the entire cortical mantle and regulates information processing in all cortical layers. Here, we recorded activity from populations of single units in the NB as rats performed a whisker-dependent tactile discrimination task. Over 80% of neurons responded with significant modulation in at least one phase of the task. Such activity started before stimulus onset and continued for seconds after reward delivery. Firing rates monotonically increased with reward magnitude during the task, suggesting that NB neurons are not indicating the absolute deviation from expected reward amounts. Individual neurons also encoded significant amounts of information about stimulus identity. Such robust coding was not present when the same stimuli were delivered to lightly anesthetized animals, suggesting that the NB neurons contain a sensorimotor, rather than purely sensory or motor, representation of the environment. Overall, these results support the hypothesis that neurons in the NB provide a value-laden representation of the sensorimotor state of the animal as it engages in significant behavioral tasks.

basal forebrain; whisker system; reward processing

OVER THE LAST 20 YEARS, IT has become clear that information processing in mammalian sensory cortices is influenced by multiple factors outside of the traditional feedforward sensory hierarchy described in the classical studies of Hubel and Wiesel (1959, 1962). Corticocortical and corticothalamic feedback (Hupe et al. 1998; Krupa et al. 1999; Lee et al. 2008; Pais-Vieira et al. 2013), subcortical neuromodulatory influences (Alenda and Nunez 2007; Aston-Jones and Cohen 2005; Lee and Dan 2012; Lin et al. 2006), attention (Gandhi et al. 1999; Steinmetz et al. 2000), behavioral context (Derdikman et al. 2006; Kleinfeld et al. 2006; Krupa et al. 2004; Nicolelis and Fanselow 2002), reward contingencies (Pantoja et al. 2007; Pleger et al. 2008), and learning (Karmarkar and Dan 2006; Weinberger 2003; Wiest et al. 2010) can significantly change processing strategies in multiple thalamocortical loops and primary sensory areas.

The nucleus basalis (NB) has been of particular interest in the study of neuromodulatory influences on cortical function, as it makes widespread, monosynaptic connections to the entire cortical mantle and the thalamus (Zaborsky et al. 2012). NB is part of the basal forebrain complex, an intricate collection of structures that form the main source of acetylcholine to the rest of the brain (Zaborsky et al. 2012). Whereas often thought of as a purely cholinergic region, it also includes GABAergic (Gritti et al. 1997), glutamatergic (Hur and Zaborszky 2005), and other projections to the cortex [see Zaborszky et al. (2012) for a review].

This expansive pattern of connectivity and neurochemical diversity allows NB to produce complex, large-scale changes in neural activity across the cortex (Berg et al. 2005; Detari et al. 1999; Metherate et al. 1992). NB is implicated in sleep-cycle transitions, suggesting a role in general vigilance or arousal (Jones 2005; Szymusiak 1995). The role of NB in attention has been an especially active area of research (Sarter et al. 2005). NB ablation consistently impairs performance in stimulus-detection tasks requiring sustained attention or vigilance (Jacobs and Juliano 1995; Muir et al. 1994, 1995), as well as selective attention (Pang et al. 1993; Voytko et al. 1994). Many NB neurons display strong responses to stimuli that are associated with rewarding or punishing stimuli (Lin and Nicolelis 2008; Richardson and DeLong 1990; Wilson and Rolls 1990). Such responses to salient stimuli are highly labile: they emerge as animals learn the relevant associations and disappear with extinction of the associations (Lin and Nicolelis 2008).

Consistent with its role in attention, NB activity significantly influences sensory processing in the cortex. For example, the stimulation of NB while presenting a visual stimulus to anesthetized cats increases signal-to-noise ratio and information rates in single primary visual cortex (V1) neurons (Goard and Dan 2009), and similar results are seen in awake, behaving mice (Pinto et al. 2013). In the somatosensory cortex, responses to tactile inputs are facilitated in the primary somatosensory cortex (S1) after NB stimulation (Howard and Simons 1994; Kuo et al. 2009; Nunez et al. 2012; Tremblay et al. 1990; Verdier and Dykes 2001; Webster et al. 1991). Some researchers have suggested that NB suppresses top-down effects on cortical function to allow more pure bottom-up sensory signals to activate primary sensory areas selectively (Ma and Luo 2012; Yu and Dayan 2005).

As mentioned above, NB activity is also strongly affected by reward (Lin and Nicolelis 2008). NB neurons do not respond equally to all rewards but show large bursts of activity to surprising rewards and negligible responses to highly predictable rewards (Lin and Nicolelis 2008). For instance, when rats received a sequence of water drops as a reward, only the first (unpredictable) drop of water elicited a burst of activity in NB, whereas subsequent (predictable) drops elicited no response

Address for reprint requests and other correspondence: M. A. Nicolelis, Box 3209, Dept. of Neurobiology, Duke Univ., Durham, NC 27710 (e-mail: nicoleli@neuro.duke.edu).

(Lin and Nicolelis 2008). Hence, NB neurons may be responsible for signaling unexpected reward events.

So far, there are no studies examining NB activity during fine-grained, whisker-based sensory discrimination in rats. We have explored extensively, at behavioral and neuronal levels, the ability of rats to discriminate between the width of different apertures using their whiskers (Krupa et al. 2001, 2004; Pais-Vieira et al. 2013; Pantoja et al. 2007; Wiest et al. 2010). This task seems a natural entry point for the study of NB dynamics and function. Data from NB neurons acquired during such tasks will allow us to begin to examine population-level NB activity in every phase of such a discrimination task and ultimately disclose the specific role of such activity in behavior, attention, and reward processing.

MATERIALS AND METHODS

For all experiments, the subjects were adult, female Long-Evans rats (250–300 g; Harlan Laboratories, Indianapolis, IN). All protocols were conducted in accord with concern for the well-being of the animals, and the Duke University Institutional Animal Use Committee approved all surgical and behavioral methods.

Behavioral training. We gathered data from the basal forebrain as rats performed an aperture-width discrimination task (Fig. 1*A*), a task that we have described in detail elsewhere (Krupa et al. 2001; Wiest et al. 2010). Briefly, rats executed the behavior in custom-built operant chambers that were controlled with MED-PC (Med Associates, St. Albans, VT). The rats were trained to discriminate behaviorally between two apertures that were different distances, along the mediolateral axis, from the face.

Rats performed this task using only information from the large facial whiskers as input (Krupa et al. 2001). Figure 1*B* shows the temporal structure of each trial: after a delay period in the reward chamber, the main door opens, allowing the rat to move into the stimulus chamber, where it samples the aperture with its whiskers and pokes its nose in a central port in the rear of the stimulus chamber. After a random delay of 100–300 ms, a tone occurs, and the rat retreats to the reward chamber. The wide and narrow apertures were initially set to 78 mm and 54 mm, respectively. Rats received reward when they poked in the left reward port for the narrower aperture and to the right for the wide aperture. The task can be made more difficult by decreasing the distance between the narrow and wide apertures. We varied the difficulty from 24 mm between the two stimuli, down to 6 mm between the stimuli. In the latter sessions, the two widths were 60 and 66 mm, respectively.

We have previously used high-speed videography to quantify whisker movements during the task (Wiest et al. 2010). In that study, we found that animals typically do not whisk but protract their whiskers until they reach the back of the stimulus chamber [as originally reported in Krupa et al. (2001)]. Because recording cables get in the way of such video analysis, we use a proxy for direct observation of contact between whiskers and the aperture: the time at which the animal breaks an infrared (IR) photobeam located on the leading edge of the aperture itself. We compared photobeam-breaking and initial whisker contact and found an extremely high correlation between the two measures (Wiest et al. 2010).

Once trained to behavioral criterion in the task (80% correct), rats were removed from water restriction for at least 4 days, followed by surgical implantation of microwire recording electrodes in the basal forebrain (see Surgical procedures below). Following at least 7 days of postsurgical recovery, rats were returned to water restriction and the behavioral task.

Whisker stimulation under anesthesia. To approximate in anesthetized rats the whisker stimulus during the aperture discrimination task, a movable aperture was swept across the rat's whiskers in a manner that simulated the whisker deflections that occurred during the active discrimination. Specifically, we matched the velocity of the moveable aperture to the velocity of the rats' movement during the aperture discrimination task. This resulted in whisker deflection dynamics that mimicked the whisker deflections that occurred during active discrimination [see Krupa et al. (2004), especially their Fig. 2*B* and online supplement]. In anesthetized recording experiments, we repeated each stimulus width a minimum of 170 times at randomized intertrial intervals between 3 and 10 s.

Surgical procedures. General procedures for chronic array implantation are defined in detail elsewhere (Wiest et al. 2008). Briefly, after anesthetizing the subject using pentobarbital, we implanted electrode arrays bilaterally in left and right basal forebrain (32 electrodes, 16 electrodes in each side). Initial electrode placement was −0.7 posterior, 2.4–2.53 medial to bregma, and −6.75 mm beneath the cortical surface (Lin and Nicolelis 2008). We recorded using in-house drivable bundles of 37-μm-diameter tungsten microwires that could be driven up to 2 mm from their initial location. We reliably measured good signals between 7 mm and 7.8 mm ventral to the cortical surface.

Neurophysiology and histology. We recorded data using the Multichannel Acquisition Processor (Plexon, Dallas, TX), with data sampled at 40 kHz. We performed spike sorting in two stages. In online sorting, we assigned spikes to units before recording the data during the task. We used a template-matching algorithm, in which waveforms that crossed a voltage threshold were first manually assigned to a putative unit to generate a mean waveform template for that unit, and then, new waveforms were assigned to the templates depending on distance from the template. In offline sorting, we used Plexon's Offline Sorter software. This involved assigning waveforms to units based on similarity of raw waveforms, clustering in principal component analysis (PCA) space, and clustering along other feature dimensions, such as the distance between a waveform's peak and valley (Fig. 1, *C* and *D*). We only counted a putative unit as a single unit if it displayed a clear, absolute, and relative refractory in the autocorrelation function (Fig. 1*E*). Furthermore, it was often the case that the same unit was registered on multiple microwires, so we used cross-correlation analysis to check for duplicates, retaining the duplicate with the higher signal to noise.

For those animals that were finished with training, we perfused with saline, followed by 10% formalin, and then acquired 40-μm coronal frozen sections and stained the sections with cresyl violet to confirm electrode placement.

PSTH analysis. We performed all further analysis in custom-written Matlab code (MathWorks, Natick, MA). We constructed peristimulus time histograms (PSTHs) with 50-ms bins for each of four epochs during the task: a baseline period between trials, the time at which animals broke an IR photobeam on the aperture to indicate stimulus onset, the onset of the tone that indicated that the animal was free to move out of the stimulus chamber, and the reward-port nose poke. We defined the baseline period as the time halfway between reward delivery and the onset of the next trial (~5 s after reward delivery). For each trial, we concatenated four individual event-related PSTHs (one corresponding to baseline, one surrounding aperture sampling, one after the tone, and one surrounding reward-port poke time) into single, full-trial PSTHs to show the temporal evolution of responses over the course of a trial (Fig. 2).

The calculation of significant deviation of PSTHs from baseline is described in more detail elsewhere (Wiest et al. 2005). Briefly, we generated a 95% confidence interval for the cumulative sum of the firing rate during the baseline period (using 2,000 bootstrap samples). Onset of a significant response was taken as the bin in which the cumulative sum fell outside of this interval. We corrected for comparisons in multiple bins using the Bonferroni correction (Zar 1996). Neurons typically had many responses during a trial (e.g., see Fig. 2), and we calculated the offset of each response as the bin at which the response fell below the 95% confidence interval (calculated using

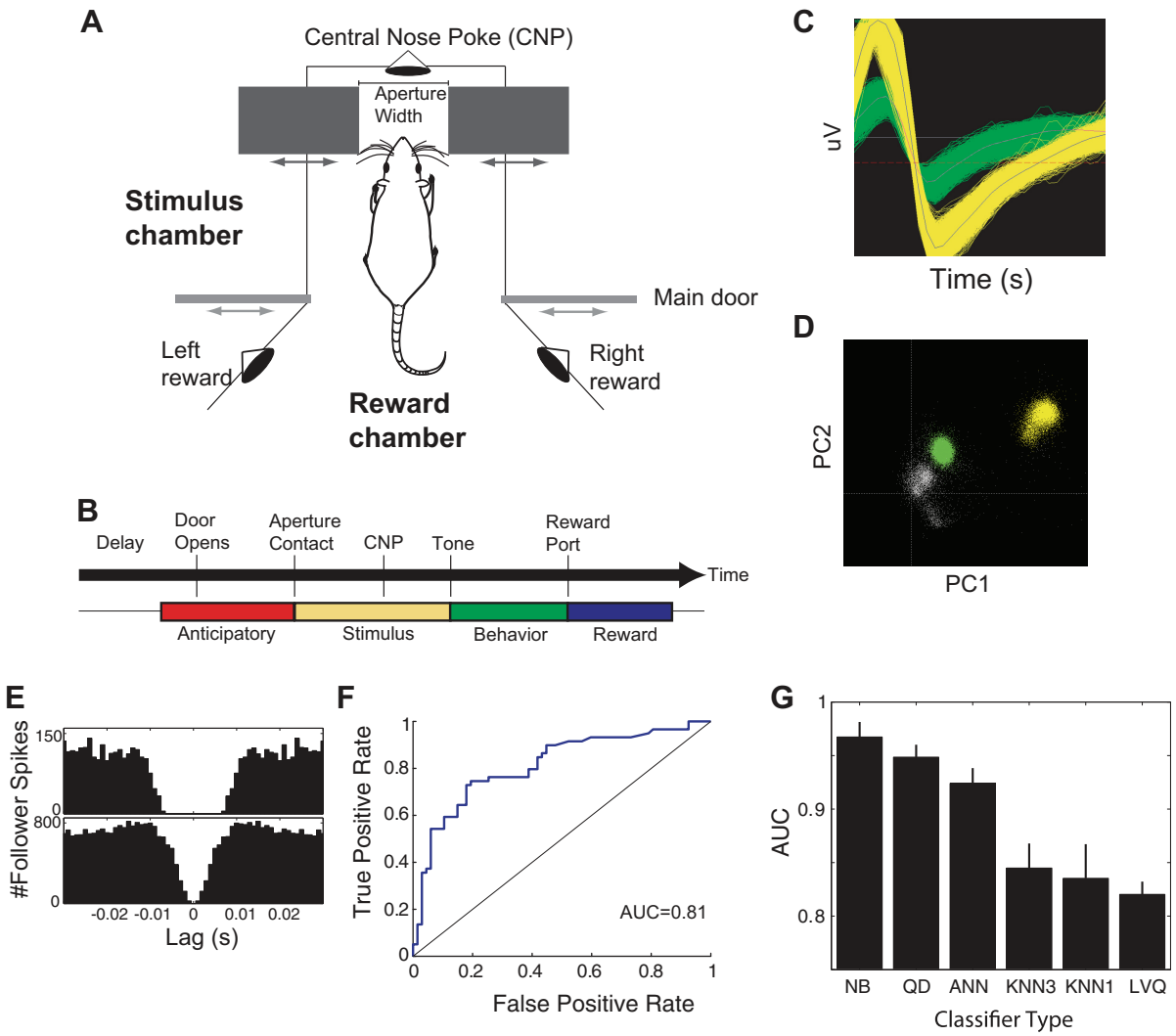

Fig. 1. Implementation of aperture-width discrimination task. *A*: schematic of the operant chamber, which consists of a reward chamber and a stimulus chamber. After the movable bars, making up the adjustable aperture, move to the correct location for a trial, the main door retracts, allowing the rat to enter the stimulus chamber, sweep its whiskers across the bars, and poke into the central nose poke (CNP). After 100–300 ms spent holding an infrared (IR) photobeam in the CNP, a tone sounds, and the animal can retreat into the stimulus chamber and poke in the right or left reward port. *B*: temporal structure of each trial, indicating anticipatory (before whisker contact), stimulus (from onset of whisker contact with the aperture), behavior (the time of the tone, indicating the animal is free to move), and reward (the time at which the animal breaks an IR photobeam in 1 of the reward ports) epochs. *C*: example of waveforms from a single channel. *D*: representation of waveforms in principal components space (PC1 and PC2) that we commonly used for offline sorting (see MATERIALS AND METHODS). Gray dots represent unsorted waveforms. *E*: autocorrelation functions from the neurons in *C*, showing clear, absolute, and relative refractory periods. *F*: example of a neuronal receiver-operating characteristic curve (ROC), calculated using a naive Bayesian (NB in *G*) classifier to estimate stimulus value (narrow/wide) based on the neuronal response of a single neuron. A curve close to the identity line (shown) is what you expect when the classifier performs at chance, and a perfect classifier will produce a value of 1 at every point on the curve. Real classifiers lie in between, and performance of a classifier can be summarized with area under the ROC (AUC), which in this example, is 0.81. *G*: mean/SE of classifier performance (AUC) for different classifiers run with 10-fold cross-validation on 1 data set with 12 neurons. QD, quadratic discriminant; ANN, 3-layer artificial neural network trained with backpropagation (10 hidden units); KNN3, k nearest neighbor with $k = 3$; KNN1, k nearest neighbor with $k = 1$; LVQ, learning vector quantization network (6 hidden units). Classifiers are ranked in descending order of mean performance.

2,000 bootstraps from the baseline period) after a significant onset event.

Neural prediction of stimuli and rewards. To measure how well single neurons could predict stimulus and reward values, we first examined performance of multiple classifiers on data from an initial benchmark data set. The benchmark data consisted of recordings from 12 neurons recorded during performance of the aperture-width discrimination task in a single session. We ran the classifier on PSTHs with bin widths ranging from 1 ms to 100 ms, and we used six different classifiers for this preliminary analysis: naive Bayes; backprop-trained, three-layer artificial neural network (ANN); k nearest neighbor (with $k = 1$ and $k = 3$); quadratic discriminant; and learning vector quantization neural network classifiers.

We performed this analysis using a freely available in-house Matlab package, called Classpack, which allows users to compare quickly the performance of multiple types of classifiers using multiple measures of performance [percent correct, mutual information, and area under the receiver-operating characteristic curve (AUC)]. In practice, all three measures were highly correlated, and we chose to report AUC measures in this study (Fig. 1*E*) (Fawcett 2006). AUC varies between 0.5 (chance) and 1.0 (perfect) performance, just like percent correct for the two-category case (Fawcett 2006). The advantages of AUC, for our study, are that its range is the same regardless of the number of categories to classify (unlike percent correct, where chance decreases with the number of categories, and unlike mutual information, where the maximum increases with the number of

categories). This invariance to category number is useful for us, because we compared classifier performance with both two and four categories (see Fig. 6*H*).

We found that the naive Bayes classifier exhibited better performance (lower variability and higher accuracy of AUC measures) than all other classifiers, even when compared with the ANN classifier over all possible numbers of hidden units (between two and 100; Fig. 1*G*). This was surprising, as naive Bayesian classifiers have known theoretical limitations, such as an inability to solve problems that are not linearly separable. However, it is also known that despite these theoretical limitations, they often work very well (and are much faster to compute) in practice (Zhang 2005), and this is what we found with our benchmark data. We found that classifier performance did not improve when bin widths were <50 ms, so we used 50-ms bin widths for all of our analyses.

To examine stimulus predictability over time during trials, we performed a moving-window analysis, examining how well 350 ms of data (corresponding to seven, 50-ms bins) could predict stimulus

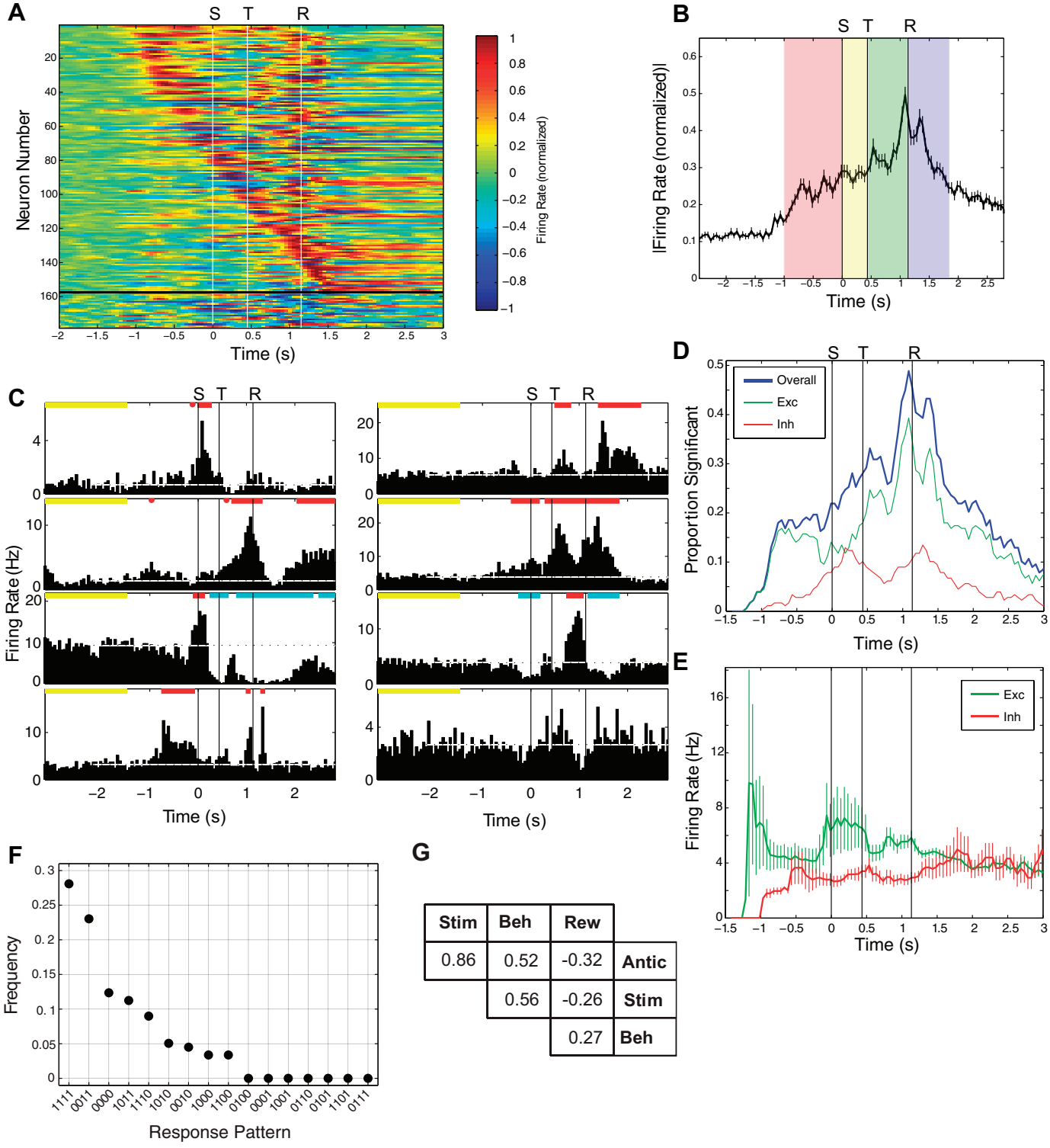

Stim	Beh	Rew	
0.86	0.52	-0.32	**Antic**
	0.56	-0.26	**Stim**
		0.27	**Beh**

value as a function of time during the trial (Fig. 3). For instance, data from before stimulus onset did not predict stimulus value, and AUC was typically near 0.5, as expected. After stimulus onset, discriminability of the stimulus increased rapidly. We performed this analysis for all 350 ms windows, shifting the window forward 100 ms with each iteration.

We took a similar approach to the analysis of how well populations of neurons predicted the stimulus and reward values. For n neurons and each 350-ms window for the analysis, we concatenated the n-relevant, seven-element PSTHs into a single vector. To preprocess the data and represent them in a lower-dimensional vector space, we performed PCA on this set of concatenated vectors. For $n > 2$, we used the scores for the first 20 components as our representation of the data. In our benchmark data, we found that increasing the number of scores beyond 20 did not help and typically, hurt classifier performance.

We ran this analysis on all possible k-tuples of neurons in each data set. This means we ran the moving-window analysis of performance n-choose-k times at each value of k (Zar 1996), for each time window. For instance, if we recorded data from $n = 12$ neurons, there would be 12-choose-four (495), four tuples to analyze; 12-choose-five (792), five tuples, etc. We performed these calculations at the Duke Shared Cluster Resource, a computer cluster that includes over 1,000 processors distributed over >80 machines, and used the Sun Grid Engine to distribute the workload to the processors.

RESULTS

General response properties. We recorded from 176 single units in NB, with recordings distributed over 33 behavioral sessions in 11 rats, as they discriminated the width of an adjustable aperture using their large facial whiskers (see MATERIALS AND METHODS and Fig. 1). This S1-dependent task requires animals to use their whiskers to discriminate the width of an adjustable aperture (i.e., narrow or wide). On each trial, the rats enter a stimulus chamber where their whiskers are deflected by the aperture. They are then required to hold their nose in a center nose poke in the rear of the stimulus chamber (Fig. 1*A*) for a variable amount of time, after which, a tone indicates that the animal is free to retreat into the reward chamber. To receive a water reward while in the reward chamber, they must select the left reward port if the aperture is narrow and the right reward port if the aperture is wide. The rats in this study performed 183 ± 12 (mean ± SE) trials/session at a percent-correct level of 86 ± 1.3.

Each trial naturally divides into four epochs: the anticipatory epoch that precedes whisker deflection; the stimulus epoch, when the whiskers are deflected by the aperture; the behavioral epoch, in which the rats retreat into the reward chamber to indicate their choice; and finally, the reward epoch, which begins when they break an IR photobeam in one of the reward ports (Fig. 1*B* and MATERIALS AND METHODS).

NB activity was significantly modulated in every epoch of the task. The mean firing rate over all neurons was 5.9 ± 0.4 Hz, and modulation of NB activity began during the anticipatory epoch, ~1 s before the onset of whisker deflection. This activity change continued for seconds after delivery of the reward (Fig. 2, *A–C*). Figure 2*A* shows the PSTHs for all neurons recorded, sorted by response latency. In 88% of neurons (155/176), activity was significantly modulated at some point during the task. During the anticipatory epoch, on average, 16% (28) of neurons showed significant modulation of activity (Fig. 2*D*). This anticipatory activity started as purely excitatory, but inhibitory activity emerged as the anticipatory epoch progressed (Fig. 2*D*). The proportion of neurons responding increased as the task progressed: on average, 25% (44) of the neurons were active during the stimulus epoch, 34% (60) during the behavioral epoch, and 39% (69) during the reward epoch.

The above numbers represent the average number of neurons active at any given time during each epoch. The average is useful for comparison because the different epochs have different durations (see Fig. 2*B*). The raw number of neurons that displayed some response over an entire epoch is much higher than the mean active over the entire epoch. For instance, 48% (85/176) showed some significant activity during the anticipatory epoch, 41% (72/176) during the stimulus epoch, 72% (126/176) during the behavioral epoch, and 63% (111/176) during the reward epoch.

There were two prominent peaks in activity associated with reward delivery. In the first, 100 ms before reward onset, 49% (86) of neurons showed significant activity. Then, 200 ms after reward onset, 43% (76) of the neurons exhibited significant activity (Fig. 2*D*). Interestingly, after NB neuronal firing modulations began, during the anticipatory epoch, the mean magnitude of change in firing rate did not change significantly throughout the remainder of the trial (Fig. 2*E*; $P > 0.6$ for both excitatory and inhibitory responses, calculated using one-way ANOVA, applied to response magnitudes at time points 1 s before stimulus onset to 1.5 s after). This constancy of activation levels was a population-level effect, as PSTHs from individual neurons showed significant variability in response magnitude over the course of the trial (see Fig. 2*C* for examples).

Figure 2*F* shows the frequency of all possible response patterns over the four epochs, with a "1" indicating a significant response and "0" no response. So, for instance, the pattern

Fig. 2. Overall structure of responses in NB. *A*: representation of peristimulus time histograms (PSTHs) from all 176 recorded neurons, sorted by time of onset of the 1st significant response during the trial. Each row represents a neuron. The PSTHs below the black horizontal line are those without significant response ($n = 21$ neurons). The 3 white vertical lines indicate stimulus onset (S), tone onset (T), and reward onset (R; denoted above the plot). Time 0 is set to be the time of stimulus onset. To aid visualization, each PSTH had the mean response before the anticipatory epoch subtracted and was then normalized to the maximum absolute value of the firing rate, so values range between −1 and 1. *B*: mean ± SE of the absolute value of all responses, from *A*, in all neurons during the task (the absolute value was used to compare deviations from baseline in both excitatory and inhibitory responses). It shows that responses typically begin ~1 s before stimulus onset. The red, yellow, green, and blue shading indicates the anticipatory, stimulus, behavior, and reward epochs, respectively. *C*: individual PSTHs from 6 neurons in the population. At the top of each panel, the yellow lines indicate the baseline period, red lines indicate times of significant excitatory responses (relative to baseline), and blue lines indicate times of significant inhibitory responses. The bottom-right PSTH is an example of a neuron without a significant deviation from baseline. *D*: proportion of neurons with significant responses as a function of time. Plot shows overall proportion of neurons responding (blue), as well as the proportion of neurons that were excited (Exc; green) and inhibited (Inh; red). *E*: mean response magnitude, calculated only for neurons with significant response modulation, as a function of time during the trial. *F*: frequency histogram of all possible binary response patterns over the 4 epochs. For instance, "0111" indicates those neurons that were significantly modulated in epochs 2–4 (stimulus, behavioral, and reward) but not anticipatory. *G*: table showing correlation coefficients among significant responses for all possible pairs of epochs. Stim, stimulus; Beh, behavioral; Rew, reward; Antic, anticipatory.

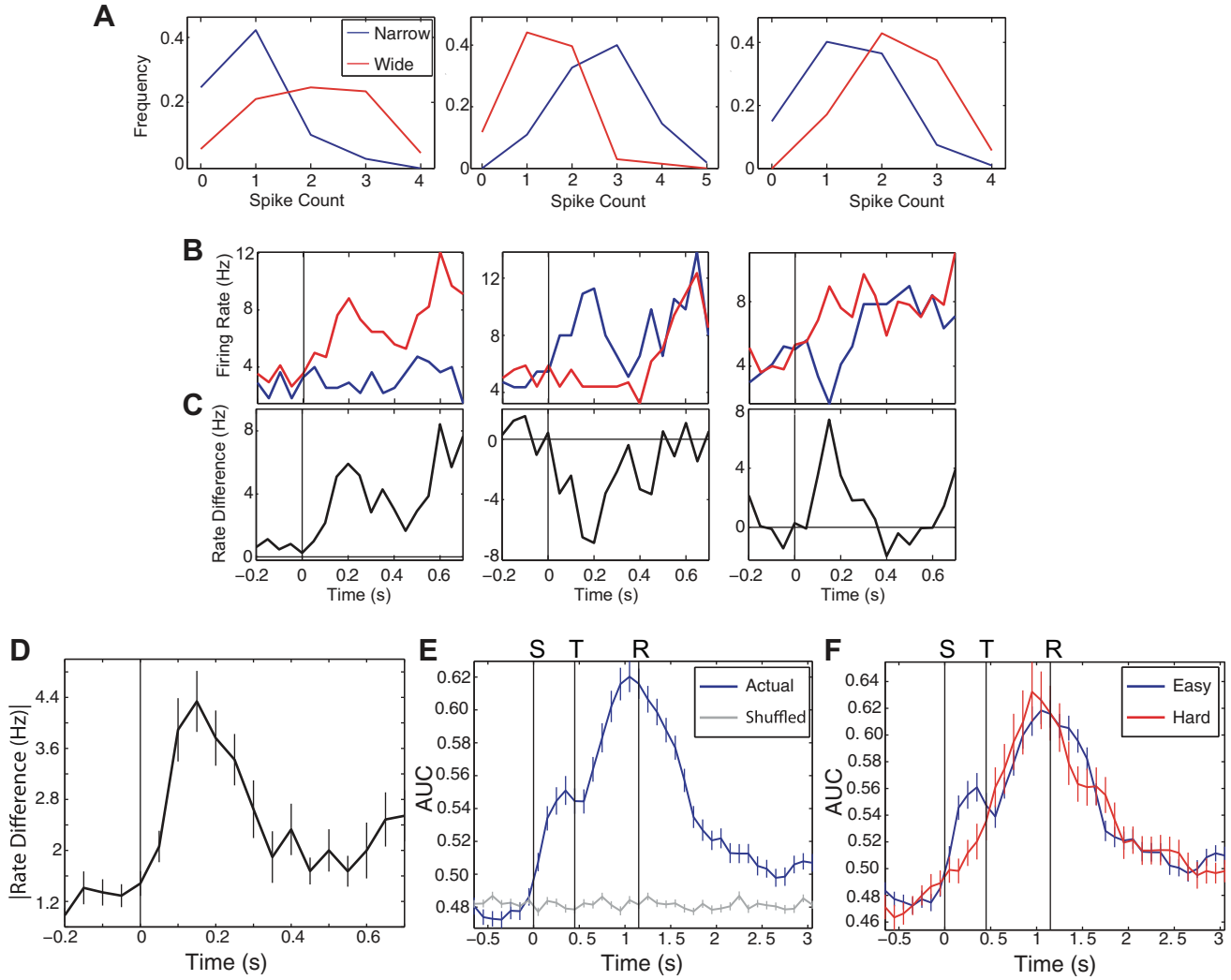

Fig. 3. Single neurons carry information about aperture width. *A*: frequency histograms of spike counts for 3 neurons in the population that showed a significantly different number of spikes in response to narrow vs. wide stimuli. *B*: PSTHs in response to narrow and wide stimuli in the same neurons as *A*, with stimulus onset at time 0 (indicated with vertical lines). *C*: difference between narrow- and wide-response PSTHs (narrow minus wide) highlights the time course of separation between the 2 stimuli. *D*: the absolute value of the difference between PSTHs for narrow and wide stimuli, calculated for all 28 neurons in which the mean count was significantly different for the 2 stimuli. *E*: moving-window analysis of classifier performance, measured as AUC, for all individual neurons. The 350-ms window was stepped forward 100 ms for the time starting −0.75 s before stimulus onset to 3 s after reward offset. Blue line shows mean ± SE of performance for all 176 individual neurons, whereas gray line shows performance when stimulus labels are shuffled. *F*: similar moving-window analysis of stimulus discrimination but with the data separated into "easy" and "hard" sessions (see MATERIALS AND METHODS and RESULTS). Easy sessions were those in which the 2 apertures were relatively far from one another, whereas for hard sessions, the apertures were relatively close together, which makes the task significantly harder for the animal.

"0011" means that a neuron's activity was not significantly modulated during the anticipatory or stimulus epochs but did show fluctuations from baseline during the behavioral and reward epochs. The most common pattern was for neuronal activity to be significantly modulated in all four epochs (38/176, or 22% of the neurons, represented as "1111" in Fig. 2*F*). The second most common response pattern was for neuronal activity to be modulated in the behavioral and reward epochs but not the anticipatory and stimulus epochs (pattern 0011, which occurred in 29/176, or 16% of neurons). The third most common pattern was for neurons to have no significant response in the four epochs (pattern "0000," which occurred in 21/176, or 12% of the neurons).

To clarify further the relationship between different activity patterns, Fig. 2*G* shows the pairwise correlations in response magnitude for all possible pairs of epochs. For example, activity during anticipatory and reward epochs tended to be negatively correlated, meaning that high anticipatory activity tends to be associated with decreased activity after reward delivery. Even though some of the correlation coefficients are low, all are significant ($P < 0.05$, *F*-test).

Note that we recorded bilaterally in NB and recorded roughly equal numbers of neurons from each side (87 from right, 89 from left). We did not observe differences in overall response proportions in the different epochs or overall firing rates in the left vs. right basal forebrain ($P > 0.05$ in all instances, using the χ^2 test for proportions and two-sided *t*-tests for differences in firing rates as a function of time). This symmetry also held for our analysis of reward- and stimulus-specific information (which we discuss next); so, in future sections, we have lumped together data from the left and right NB.

Stimulus and behavioral epochs. Whereas activity in many NB neurons was significantly modulated during the stimulus epoch, did such responses carry stimulus-specific information? We examined responses to narrow vs. wide stimuli for each neuron in the stimulus epoch, between 0 and 350 ms after the onset of whisker deflection. A total of 28/176 (16%) of the neurons showed a significant difference in the mean number of spikes produced in this window on narrow vs. wide trials ($P < 0.05$, two-tailed *t*-test). Figure 3*A* shows representative frequency histograms of spike counts in response to wide vs. narrow apertures, and the raw PSTHs show the different time-varying firing rates for the same examples (Fig. 3*B*).

The time course of the difference between the responses to wide and narrow stimuli is shown in Fig. 3*C*. The population-level difference in firing rate is illustrated in Fig. 3*D*, which shows the mean difference between the wide and narrow PSTHs for all of those neurons with a significantly different mean spike count for the two stimuli. Of the 28 neurons with significant differences in mean spike count, 64% (18/28) responded with more spikes to narrow stimuli, and 36% (10/28) preferred the wide aperture, a significant difference in proportion ($P = 0.03$, χ^2 test).

To quantify how much stimulus-specific information was carried in NB, we performed a moving-window analysis of how well NB neurons discriminated aperture width as a function of time. Specifically, for the time period lasting from 1 s before stimulus onset to 3 s after reward offset, we used a naive Bayesian classifier to predict the aperture width based on activity in each neuron. We used the AUC to measure the classifier's ability to predict the stimulus (see MATERIALS AND METHODS). We analyzed stimulus discriminability in all 350-ms windows within this time period and shifted this 350-ms window forward in time in 100-ms increments to give a fine-grained readout of discrimination. Figure 3*E* shows the mean performance for all neurons, illustrating that individual NB neurons undergo a rapid increase in information about the stimulus after stimulus onset, with an initial, prominent bump 350 ms after stimulus onset (Fig. 3*E*).

Surprisingly, NB neurons also predicted stimulus value through the remainder of a trial, from stimulus onset through the reward epoch. In fact, maximum discrimination was reached just before the reward epoch (Fig. 3*E*), the time at which the largest proportion of NB neurons exhibited a significant deviation from their baseline firing (recall Fig. 2*D*). This is likely explained by the fact that animals displayed gross behavioral differences for narrow and wide trials during the behavioral epoch, and NB neurons are known to respond differently when an animal exhibits different behaviors (Mitchell et al. 1987; Richardson and DeLong 1990; Szymusiak et al. 2000).

As we would expect for neurons encoding sensory information, NB neurons are better at discriminating two apertures that are far apart than two apertures that are close together. To examine this, we separated the behavioral sessions into those in which the discrimination task was relatively easy (the two apertures were >18 mm apart: 23 sessions, 133 neurons) and those in which it was harder (the apertures were <11 mm apart, making the discrimination task more difficult: 10 sessions, 43 neurons). To decrease the chance of behavioral contamination of sensory response, we examined sensory discrimination in easy and hard sessions only during the sensory epoch for the PSTH between 50 ms and 350 ms after stimulus onset. Figure 3*F* reveals a significantly higher discrimination of aperture width during the sensory epoch for the easier sessions ($P = 0.01$, two-tailed *t*-test applied to performance, 350 ms after onset of the stimulus epoch).

To determine the likelihood that the differential responses to different stimuli were the result of feedforward sensory processing, without interactions from factors such as attention or behavior, we recorded NB responses to whisker deflections under light isoflurane anesthesia in 29 neurons in two animals (four sessions). The whiskers of the anesthetized animals were contacted with sliding bars set up to deflect their whiskers, so as to mimic closely whisker stimulation produced during performance of the aperture-width discrimination task in awake animals (Krupa et al. 2004). The majority (69%; 20/29) of NB neurons in anesthetized animals showed significant sensory response to whisker deflections (Fig. 4, *A* and *B*).

Despite the presence of this vigorous population-level response to two widths that animals could easily discriminate when awake, we observed negligible stimulus-specific information in single NB neurons in anesthetized animals. None of the neurons showed different spike counts for narrow vs. wide stimuli, and Fig. 4*C* shows the impoverished classifier performance in anesthetized animals compared with what we observed in awake animals.

Note that in the analysis of stimulus discrimination in awake animals, we included only correct trials, so stimulus and behavior were correlated perfectly (e.g., on correct trials, when the stimulus is narrow, the animals always move to the left). To differentiate information about stimulus and behavior, we performed additional analysis of activity from the same sessions.

For one such analysis, we held the behavior constant by restricting our analysis to those trials in which the animal chose one reward port (e.g., the left reward port). This subset of data included both correct trials (the stimulus was narrow) and incorrect trials (the stimulus was wide). We applied the same classifier analysis as above to predict stimulus value in constant-behavior trials, in a small time window surrounding the stimulus epoch (Fig. 4*D*). Classifier performance vs. time in the stimulus epoch is illustrated, showing a negligible increase in performance in the window ending 350 ms after stimulus onset. For comparison, classifier performance of the individual neurons on correct trials from Fig. 3, which is significantly higher (see below), is also shown.

Based on these results, we expected that most of the putatively stimulus-specific information was actually due to subtle behavioral differences, such as different whisker movements, on narrow and wide trials. To test this hypothesis, we then restricted our analysis to all trials in which the same stimulus was presented (e.g., narrow) and used the classifier to predict which of two behaviors the animal displayed: left (for correct trials) or right (for incorrect trials). This analysis is not an analysis of sensory coding, but of behavioral coding, or how well the neural activity in NB predicts differences in the animal's behavior when the stimulus is held constant.

Surprisingly, the behavioral discrimination curve (Fig. 4*D*) is not significantly different from the "pure" sensory discrimination curve ($P > 0.05$, two-sided *t*-test for all points on the curve, with Bonferroni correction). Both curves are significantly lower than that observed with correct trials only (Fig. 4*D*). Furthermore, the discrimination of stimuli on correct trials is greater than the sum of the pure sensory and behavioral

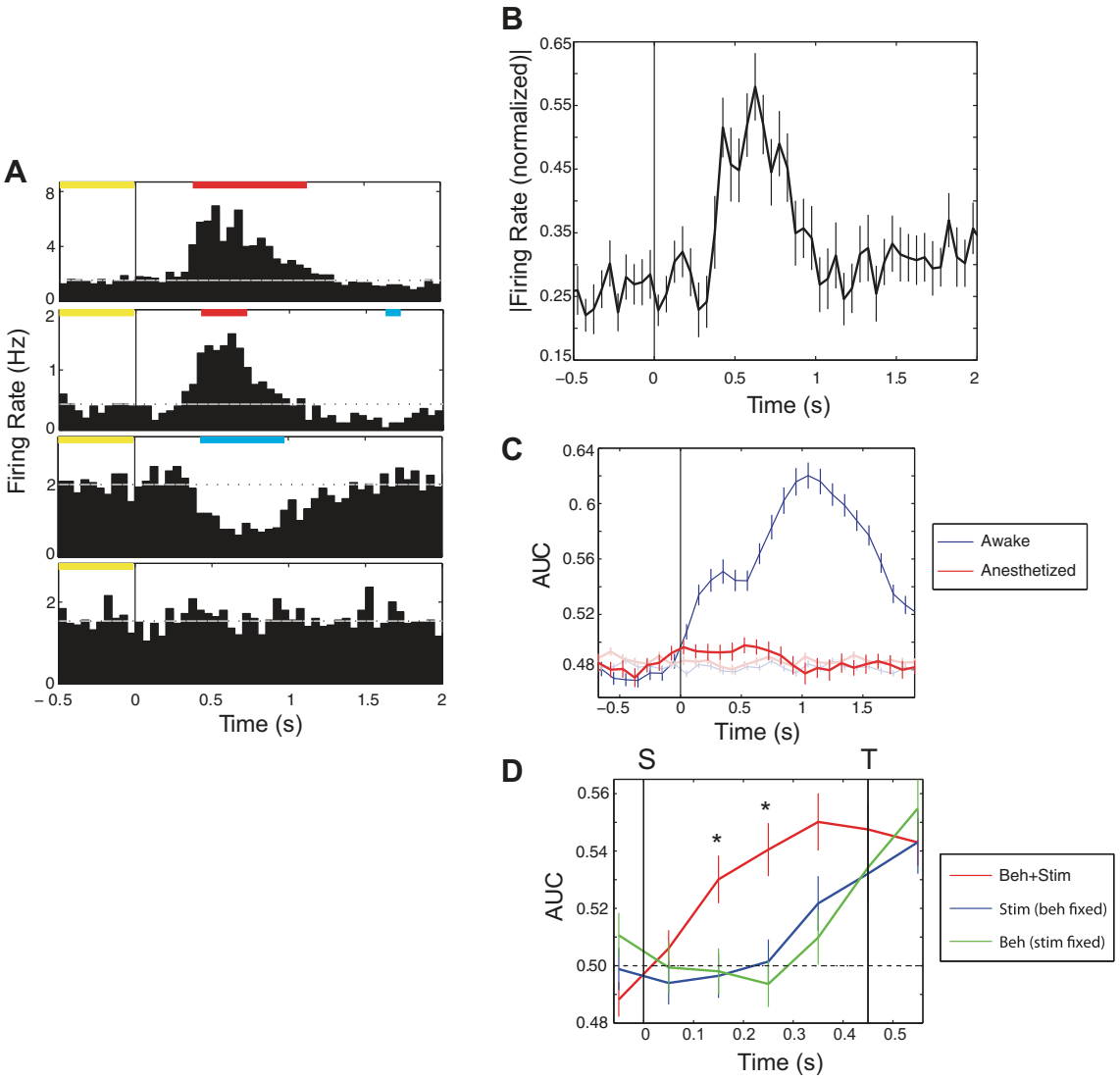

Fig. 4. Single neuron responses to whisker deflection in NB of anesthetized animals. *A*: individual PSTHs from 4 neurons in the population. Conventions are the same as in Fig. 2*C*. *B*: normalized PSTH for all 29 single units recorded in anesthetized animals (same conventions as in Fig. 2*B*). *C*: as in Fig. 3*E*, classifier performance, measured as AUC, for all individual neurons (red), with performance in awake animals during the task shown for reference (blue). The light blue and light red traces are classifier performance when stimulus labels are shuffled. *D*: discrimination of stimuli and behavior during the stimulus epoch. Blue line shows classifier performance vs. time when analysis is extended to trials in which behavior is the same (e.g., left), and the classifier must predict stimulus value. The green line shows performance when the classifier predicts behavior when the stimulus is held constant (e.g., only narrow trials from a session). The red line shows classifier performance on correct trials, presented in Fig. 3, in which stimulus and behavior are perfectly correlated. Asterisks indicate time points at which the above-chance performance of the classifier on correct trials is larger than the sum of the above-chance classifier performance in the behavior-fixed and stimulus-fixed cases.

discrimination curves ($P < 0.05$, one-sided *t*-test with Bonferroni correction).

Cumulatively, the above results suggest that the discrimination of aperture width in NB emerges from a nonlinear interaction between behavioral and sensory processes (see DISCUSSION). That is, whereas NB neurons respond to whisker deflections, even in anesthetized animals, the differential responses observed during the task seem to be sensorimotor in nature [as also suggested by data from monkeys (Richardson and DeLong 1990); see DISCUSSION].

Because we recorded from multiple NB neurons during the task (between one and 15 units, with a mean of 5.3 units/recording session), we were able to examine the encoding of such sensorimotor information in populations of NB neurons. We again applied a moving-window analysis with a classifier to predict which aperture width was presented during each trial. However, for the population analysis, we applied the classifier to 350 ms windows with data combined from all possible combinations of neurons in each session. For instance, in a data set in which we recorded from 13 neurons, we analyzed how much information was contained about the aperture in all 1,287 groups of five neurons, all 1,716 groups of six neurons, etc. (see MATERIALS AND METHODS). Figure 5*A* shows the result of such an analysis from a session in which we recorded from 13 neurons simultaneously. This analysis revealed a clear and rapid increase in sensorimotor information with the addition of more neurons.

To quantify the amount of information in the sensory epoch as a function of the number of neurons in the population, we plotted AUC vs. number of neurons for the 350-ms window

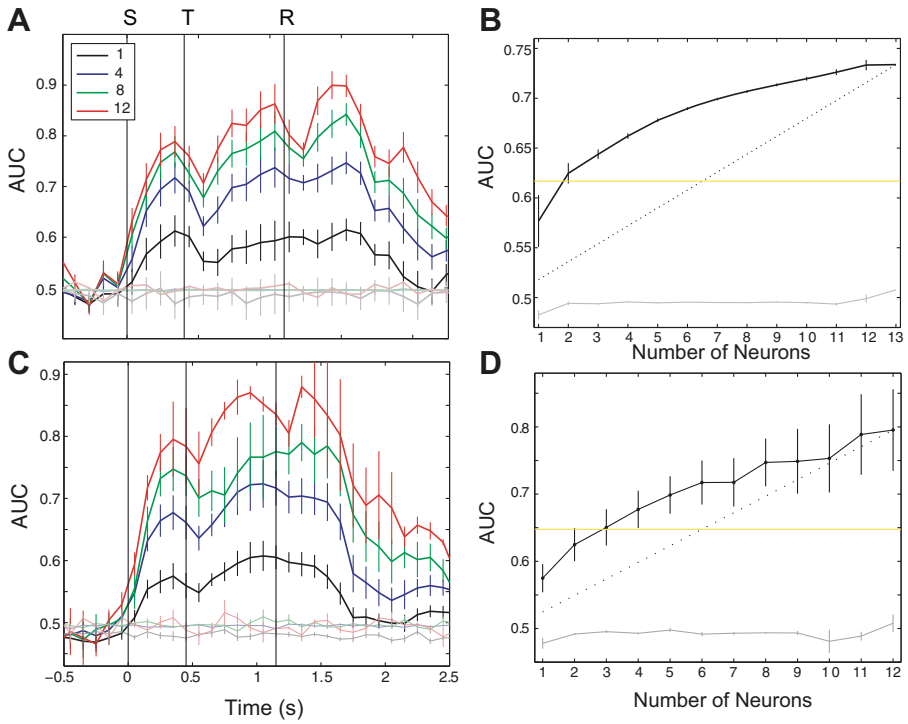

Fig. 5. Population-level sensory discrimination. *A*: population moving-window analysis of aperture-width prediction from a single session in which we recorded from 13 neurons. Each trace shows the mean ± SE AUC for all possible groups of k neurons, for $k = 1$, 4, 8, and 12. The lighter lines show performance when the classifier was applied to data with stimulus labels shuffled. *B*: mean ± SE AUC for the window between 0 and 350 ms after stimulus onset, as a function of number of neurons included in the response. The curve illustrates how sensory discrimination during the sensory epoch increases with number of neurons in the population. The yellow line indicates the performance that is halfway between chance (0.5) and the maximum for the population (0.72). The dashed line shows what the curve would look like if each neuron made the same contribution to performance. *C*: same conventions as in *A*, but the plot shows the mean performance over all 8 sessions in which we recorded from 5 or more neurons. *D*: same conventions as in *B* but showing mean performance over all sessions represented in *C*. Note that the SE increases with number of neurons because there are fewer sessions with larger numbers of neurons.

after stimulus onset (Fig. 5*B*). This revealed a rapidly saturating curve, such that, on average, the classifier performed half as well as the entire population by simply using two neurons. This indicates a high level of redundancy in the coding scheme.

We observed similar results after averaging performance over multiple sessions. Figure 5*C* shows the average moving-window performance over the eight sessions in three rats in which we recorded five or more neurons simultaneously. Figure 5*D* shows the mean classifier performance in the 350-ms window after stimulus onset, averaged over the same eight sessions. Whereas less pronounced, we still see a rapid saturating curve, again suggesting a coding scheme with significant redundancy.

Reward epoch. We next examined modulation of NB activity during the reward epoch, when the animals poked their noses in the reward port to receive reward (Fig. 1*A*). During the sessions, it was possible to hear rapid-fire bursts of spikes, via the audio monitor, just before the animals selected a reward port. This typical profile is reflected in Fig. 6*A*, which shows the mean PSTH in response to reward for both correct and incorrect trials. Note the sharp rise before reward onset in both conditions and the drop in activity when no reward is delivered. The mean difference in PSTH for rewarded and unrewarded trials is shown in Fig. 6*B*.

In 24 sessions (115 neurons), we varied the amount of reward delivered on different trials, giving four different amounts of water: none (incorrect trials) and low, medium, and high reward amounts for correct trials. The medium volume was the mean of the low and high volumes delivered. Overall, 58% (66/114) of the neurons displayed different spike counts to the four different levels of reward ($P < 0.05$, ANOVA). Figure 6*C* shows the frequency histograms of spike count for each reward value for three neurons, and the corresponding peri-reward time histograms are shown in Fig. 6*D*. Figure 6*E* displays the mean peri-reward time histograms for the four reward magnitudes, for those neurons with a significantly different number of spikes evoked by the four rewards. It illustrates the observed response suppression for lower reward values and boosted activity for higher reward magnitudes.

Figure 6*F* shows the mean spike counts for each reward value in the 350-ms window after reward delivery. Qualitatively, NB neurons seemed to split their responses into two coarse categories: "low," which included zero and low rewards, and "high," which included medium and high reward levels. For those NB neurons that showed significantly different responses to the four reward values, we performed a post hoc analysis of which response pairs were significantly different. The table in Fig. 6*G* shows the results of this analysis. For instance, a relatively low proportion (0.18) of neurons exhibited different responses to zero and low reward values, whereas a high proportion (0.88) showed significantly different responses to low and high rewards.

We quantified how much information that NB neurons transmitted about reward magnitude using the same moving-window analysis that we used for the analysis of stimulus-specific information. Figure 6*H* shows that individual NB neurons discriminated among reward values with high accuracy. On average, the AUC was 0.65 ± 0.05 for individual neurons 500 ms after the reward port was poked by the rat. This was significantly higher than the ability of the same group of neurons to discriminate aperture width, which is superimposed for comparison ($P = 1e\text{-}9$, two-tailed t-test).

To determine the correlation between reward encoding and stimulus encoding in single neurons, we calculated the correlation coefficient between classifier performance on aperture prediction in the window ending 350 ms after stimulus onset and classifier performance on reward prediction in the window ending 500 ms after reward onset. The correlation between classifier performance for stimulus and reward discrimination, over all neurons, was small ($r = 0.2$) although significant ($P = 2 \times 10^{-4}$, F-test; see DISCUSSION).

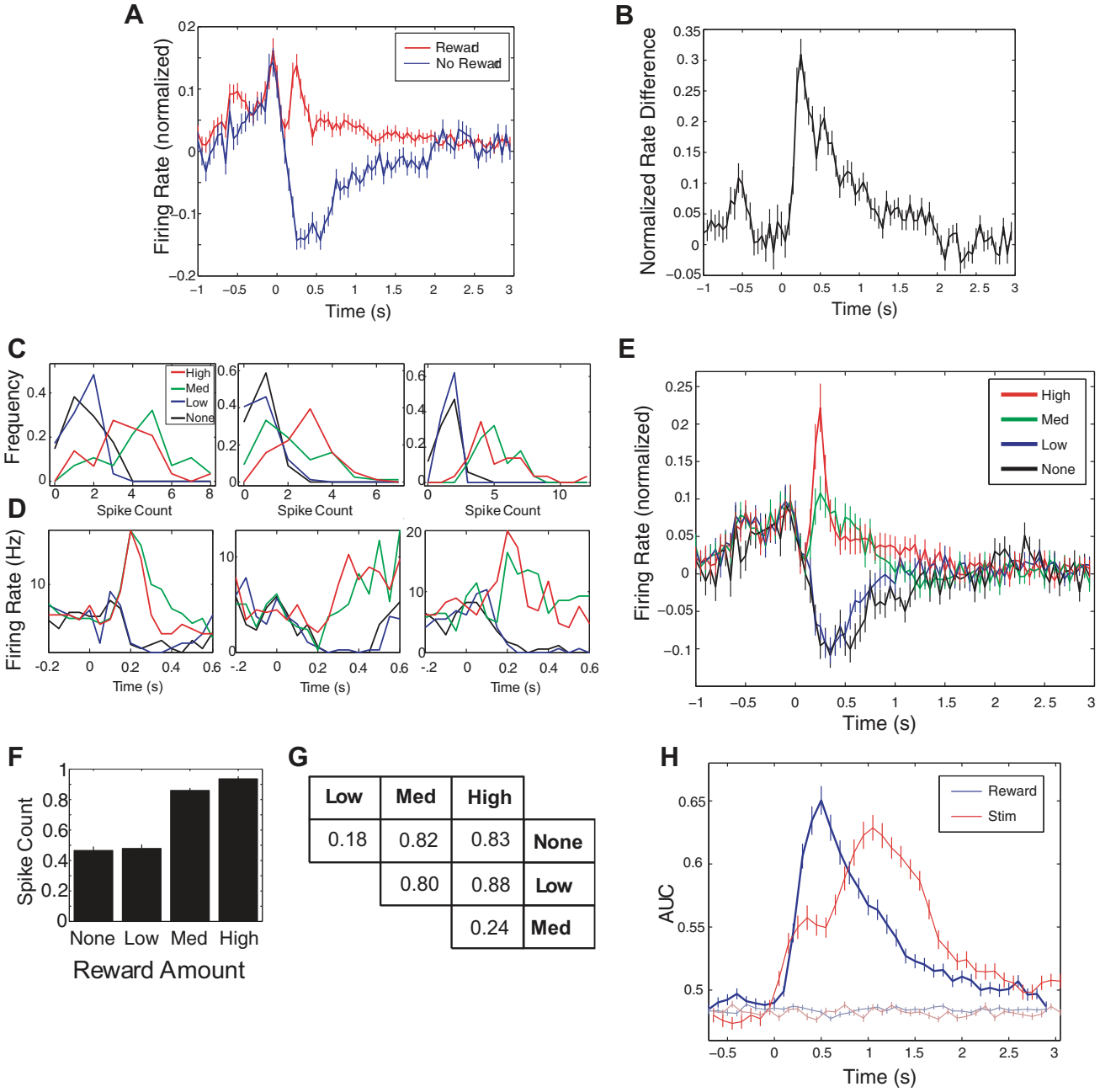

Fig. 6. Reward dependence of responses in NB neurons. *A*: mean ± SE of the response to all trials with (red) and without (blue) rewards, where time 0 is the time of reward delivery (n = 176 neurons). For each neuron, the baseline firing rate was subtracted, and firing rate was normalized to the maximum absolute value of firing rate. *B*: difference between rewarded and unrewarded trials averaged over all neurons. *C*: frequency histograms of spike counts for the 22 sessions in which the rats received 4 different reward values (where incorrect trials are counted as "None"). *D*: peri-reward time histograms for the same neurons depicted in *C*. *E*: population mean ± SE of responses to 4 reward amounts, where the mean is over the firing rates, normalized to the maximum as before. *F*: mean ± SE spike count over all neurons from sessions with 4 reward values (counts calculated in the 500-ms window after reward onset and normalized to the maximum spike count for each neuron). *G*: table showing proportion of neurons with different spike counts in response to different reward amounts. Analysis is post hoc, only performed on those neurons that already tested positive for a difference in spike count (see RESULTS). *H*: moving-window analysis applied to prediction of reward in single neurons for those sessions with 4 reward magnitudes. The blue line is mean ± SE of the AUC when the naive Bayesian classifier was used to predict reward amount. The red line is the classifier performance for stimulus prediction, shifted to overlap in time with the reward predictor, for the same group of neurons. The lighter lines are the results when the same analysis is applied with reward values shuffled.

DISCUSSION

We showed that populations of NB neurons display significant firing-rate modulations that lasted for the duration of individual trials as rats performed a tactile discrimination task. During a typical trial, such modulations began ~1 s before the onset of mechanical deflection of the whiskers and persisted for >3 s after reward delivery (Fig. 2). The modulation of activity before whisker deflection is particularly interesting, as we have observed such anticipatory activity in the entire somatosensory processing stream [including cortical areas S1 and primary motor (M1) and thalamic nuclei ventral posteromedial (POM) and POM]

during the aperture-width discrimination task (Krupa et al. 2004; Pais-Vieira et al. 2013; Wiest et al. 2010).

Our findings suggest that NB is an important component of a broadly distributed cortical-subcortical circuit that defines the animal's expectations about the task. In the future, it would be interesting to determine the effects of NB inactivation on anticipatory activity in the somatosensory system. It will be crucial, in future studies, to supplement our functional studies with information about which cell types (cholinergic, GABAergic, or others) we are recording from in NB to help us better develop specific models of NB influence on cortical function.

The NB is not a simple, well-localized nucleus but a diffuse and complex structure, spanning ~4 mm along the rostrocaudal axis (Johnson et al. 2012; Paxinos and Watson 2007), with topographically organized projections to the cortex (Zaborszky et al. 2013). For instance, NB neurons in the caudal NB project more to auditory cortex, and more rostral cells project to the somatosensory cortex (Baskerville et al. 1993; Bigl et al. 1982; Lamour et al. 1982; McKinney et al. 1983; Saper 1984). It would be very interesting, in future studies, to examine NB dynamics in multiple locations during the aperture-width discrimination task. We chose one location based on previous work (Lin and Nicolelis 2008), but it would be interesting to determine how much variability there is in the population-level response patterns.

NB neuronal activity was very strongly modulated by reward anticipation and reward amounts. Almost one-half of NB neurons exhibited bursts of firing just before the animal poked in the reward ports (Fig. 2*D*). Moreover, NB activity was strongly dependent on reward magnitude (Fig. 6).

A previous study showed that NB neurons responded strongly to unexpected rewards but exhibited no change in activity in response to highly predictable rewards (Lin and Nicolelis 2008). Whereas the previous study varied reward predictability within sessions, while keeping reward constant, we took a complementary approach. Namely, within each session, we kept the predictability of the reward constant while varying reward amounts. This allowed us to test the hypothesis that NB activity would be proportional to absolute deviation from the mean reward amount, in which case, we would see relatively large responses to both high and low reward magnitudes. The alternate hypothesis was that NB responses would be directly proportional to reward magnitude. We found clear evidence of the latter, i.e., NB response magnitude increased monotonically with reward magnitude (Fig. 6). This suggests that when the predictability of the reward is kept constant, NB activity is proportional to raw reward magnitude. Such temporally structured reward signals likely help explain the powerful role of NB activity in learning and cortical plasticity (Bear and Singer 1986; Chubykin et al. 2013; Kilgard and Merzenich 1998).

As a population, NB neurons responded during every significant event during a task trial, a result that supports previous research, suggesting an important role for this forebrain structure in general vigilance or arousal (Oken et al. 2006). Furthermore, NB neuronal populations carried significant information about the specific sensorimotor patterns executed on each trial. To determine whether such responses enhance cortical processing of tactile stimuli, we could attempt to manipulate the activity of NB neurons and determine the effects on behavior and processing in S1. For instance, we might give twice as much reward when the stimulus is wide. Based on previous research (Lin and Nicolelis 2008; Weinberger 2003), we strongly expect NB neurons to become preferentially activated by the wide aperture (Lin and Nicolelis 2008), thereby enhancing the difference in response, in NB, to the two stimuli. We would expect this to be reflected in a behavioral bias in the task, such that the animal will come to respond as if the more rewarded stimulus occurred with a higher frequency. We could easily measure the correlation between the emergence of the behavioral bias and the emergence of the differential responses in NB.

In lightly anesthetized animals, most NB neurons showed significant responses to whisker deflection (Fig. 4, *A* and *B*). Despite such responses, NB neurons in anesthetized animals carried negligible stimulus-specific information about aperture width, even though we used tactile stimuli that animals could easily discriminate when awake (Fig. 4*C*). This suggests that sensorimotor information is routed to NB only when animals are attentively engaged in an active discrimination task. This is likely because the inputs to NB from the frontal lobe are disrupted with anesthesia (Imas et al. 2005; Laplante et al. 2005; Rasmusson et al. 2007), and there likely exist subtle behavioral differences on wide and narrow trials during the stimulus epoch, differences that could influence NB activity (Szymusiak et al. 2000). It will be useful to record from NB neurons during the task when somatosensory thalamus or cortex is inactivated to disentangle more conclusively sensory and motor effects within NB than we have in this study.

We know that NB is made up of an extremely anatomically and chemically heterogeneous set of neurons (Zaborsky et al. 2012). Our data reflect the corresponding functional heterogeneity of this region of the forebrain. We did not find that individual neurons encoded information about every relevant aspect of the task while others sat idle or that individual neurons only responded to single events during the task. Rather, our data suggest that NB neurons encode multiple aspects of the important dimensions of the full behavior with different ensembles forging temporary coalitions to produce an ongoing, value-laden representation of the animals' behavior and environment as they navigate their world.

ACKNOWLEDGMENTS

We thank A. Huh and E. Lehew for help in training animals; G. Lehew and J. Meloy for help in building the experimental setup and recording electrodes; and S. Halkiotis for help in preparing the manuscript. We also thank Shih Chieh Lin for commentary on the paper and Konstantin Hartmann for helping with final edits.

GRANTS

Support for this work was provided by the National Institute of Dental and Craniofacial Research (RO1 DE-011451 to M. A. Nicolelis).

DISCLOSURES

The authors declare no competing financial interests. The content is solely the responsibility of the authors and does not necessarily represent the official views of the NIH.

AUTHOR CONTRIBUTIONS

Author contributions: E.T., J.L., and M.A.N. conception and design of research; E.T., J.L., K.S., A.M., and S.T. performed experiments; E.T. ana-

lyzed data; E.T. and M.A.N. interpreted results of experiments; E.T. prepared figures; E.T. and M.A.N. drafted manuscript; E.T. and M.A.N. edited and revised manuscript; E.T. and M.A.N. approved final version of manuscript.

REFERENCES

Alenda A, Nunez A. Cholinergic modulation of sensory interference in rat primary somatosensory cortical neurons. *Brain Res* 1133: 158–167, 2007.

Aston-Jones G, Cohen JD. An integrative theory of locus coeruleus-norepinephrine function: adaptive gain and optimal performance. *Annu Rev Neurosci* 28: 403–450, 2005.

Baskerville KA, Chang HT, Herron P. Topography of cholinergic afferents from the nucleus basalis of Meynert to representational areas of sensorimotor cortices in the rat. *J Comp Neurol* 335: 552–562, 1993.

Bear MF, Singer W. Modulation of visual cortical plasticity by acetylcholine and noradrenaline. *Nature* 320: 172–176, 1986.

Berg RW, Friedman B, Schroeder LF, Kleinfeld D. Activation of nucleus basalis facilitates cortical control of a brain stem motor program. *J Neurophysiol* 94: 699–711, 2005.

Bigl V, Woolf NJ, Butcher LL. Cholinergic projections from the basal forebrain to frontal, parietal, temporal, occipital, and cingulate cortices: a combined fluorescent tracer and acetylcholinesterase analysis. *Brain Res Bull* 8: 727–749, 1982.

Chubykin AA, Roach EB, Bear MF, Shuler MG. A cholinergic mechanism for reward timing within primary visual cortex. *Neuron* 77: 723–735, 2013.

Derdikman D, Yu C, Haidarliu S, Bagdasarian K, Arieli A, Ahissar E. Layer-specific touch-dependent facilitation and depression in the somatosensory cortex during active whisking. *J Neurosci* 26: 9538–9547, 2006.

Detari L, Rasmusson DD, Semba K. The role of basal forebrain neurons in tonic and phasic activation of the cerebral cortex. *Prog Neurobiol* 58: 249–277, 1999.

Fawcett T. An introduction to ROC analysis. *Pattern Recogn Lett* 27: 861–874, 2006.

Gandhi SP, Heeger DJ, Boynton GM. Spatial attention affects brain activity in human primary visual cortex. *Proc Natl Acad Sci USA* 96: 3314–3319, 1999.

Goard M, Dan Y. Basal forebrain activation enhances cortical coding of natural scenes. *Nat Neurosci* 12: 1444–1449, 2009.

Gritti I, Mainville L, Mancia M, Jones BE. GABAergic and other noncholinergic basal forebrain neurons, together with cholinergic neurons, project to the mesocortex and isocortex in the rat. *J Comp Neurol* 383: 163–177, 1997.

Howard MA 3rd, Simons DJ. Physiologic effects of nucleus basalis magnocellularis stimulation on rat barrel cortex neurons. *Exp Brain Res* 102: 21–33, 1994.

Hubel DH, Wiesel TN. Receptive fields, binocular interaction and functional architecture in cats visual cortex. *J Physiol* 160: 106–154, 1962.

Hubel DH, Wiesel TN. Receptive fields of single neurones in the cat's striate cortex. *J Physiol* 148: 574–591, 1959.

Hupe JM, James AC, Payne BR, Lomber SG, Girard P, Bullier J. Cortical feedback improves discrimination between figure and background by V1, V2 and V3 neurons. *Nature* 394: 784–787, 1998.

Hur EE, Zaborszky L. Vglut2 afferents to the medial prefrontal and primary somatosensory cortices: a combined retrograde tracing in situ hybridization study [corrected]. *J Comp Neurol* 483: 351–373, 2005.

Imas OA, Ropella KM, Ward BD, Wood JD, Hudetz AG. Volatile anesthetics disrupt frontal-posterior recurrent information transfer at gamma frequencies in rat. *Neurosci Lett* 387: 145–150, 2005.

Jacobs SE, Juliano SL. The impact of basal forebrain lesions on the ability of rats to perform a sensory discrimination task involving barrel cortex. *J Neurosci* 15: 1099–1109, 1995.

Johnson GA, Calabrese E, Badea A, Paxinos G, Watson C. A multidimensional magnetic resonance histology atlas of the Wistar rat brain. *Neuroimage* 62: 1848–1856, 2012.

Jones BE. From waking to sleeping: neuronal and chemical substrates. *Trends Pharmacol Sci* 26: 578–586, 2005.

Karmarkar UR, Dan Y. Experience-dependent plasticity in adult visual cortex. *Neuron* 52: 577–585, 2006.

Kilgard MP, Merzenich MM. Cortical map reorganization enabled by nucleus basalis activity. *Science* 279: 1714–1718, 1998.

Kleinfeld D, Ahissar E, Diamond ME. Active sensation: insights from the rodent vibrissa sensorimotor system. *Curr Opin Neurobiol* 16: 435–444, 2006.

Krupa DJ, Ghazanfar AA, Nicolelis MA. Immediate thalamic sensory plasticity depends on corticothalamic feedback. *Proc Natl Acad Sci USA* 96: 8200–8205, 1999.

Krupa DJ, Matell MS, Brisben AJ, Oliveira LM, Nicolelis MA. Behavioral properties of the trigeminal somatosensory system in rats performing whisker-dependent tactile discriminations. *J Neurosci* 21: 5752–5763, 2001.

Krupa DJ, Wiest MC, Shuler MG, Laubach M, Nicolelis MA. Layer-specific somatosensory cortical activation during active tactile discrimination. *Science* 304: 1989–1992, 2004.

Kuo MC, Rasmusson DD, Dringenberg HC. Input-selective potentiation and rebalancing of primary sensory cortex afferents by endogenous acetylcholine. *Neuroscience* 163: 430–441, 2009.

Lamour Y, Dutar P, Jobert A. Topographic organization of basal forebrain neurons projecting to the rat cerebral cortex. *Neurosci Lett* 34: 117–122, 1982.

Laplante F, Morin Y, Quirion R, Vaucher E. Acetylcholine release is elicited in the visual cortex, but not in the prefrontal cortex, by patterned visual stimulation: a dual in vivo microdialysis study with functional correlates in the rat brain. *Neuroscience* 132: 501–510, 2005.

Lee S, Carvell GE, Simons DJ. Motor modulation of afferent somatosensory circuits. *Nat Neurosci* 11: 1430–1438, 2008.

Lee SH, Dan Y. Neuromodulation of brain states. *Neuron* 76: 209–222, 2012.

Lin SC, Gervasoni D, Nicolelis MA. Fast modulation of prefrontal cortex activity by basal forebrain noncholinergic neuronal ensembles. *J Neurophysiol* 96: 3209–3219, 2006.

Lin SC, Nicolelis MA. Neuronal ensemble bursting in the basal forebrain encodes salience irrespective of valence. *Neuron* 59: 138–149, 2008.

Ma M, Luo M. Optogenetic activation of basal forebrain cholinergic neurons modulates neuronal excitability and sensory responses in the main olfactory bulb. *J Neurosci* 32: 10105–10116, 2012.

McKinney M, Coyle JT, Hedreen JC. Topographic analysis of the innervation of the rat neocortex and hippocampus by the basal forebrain cholinergic system. *J Comp Neurol* 217: 103–121, 1983.

Metherate R, Cox CL, Ashe JH. Cellular bases of neocortical activation: modulation of neural oscillations by the nucleus basalis and endogenous acetylcholine. *J Neurosci* 12: 4701–4711, 1992.

Mitchell SJ, Richardson RT, Baker FH, DeLong MR. The primate nucleus basalis of Meynert: neuronal activity related to a visuomotor tracking task. *Exp Brain Res* 68: 506–515, 1987.

Muir JL, Everitt BJ, Robbins TW. AMPA-induced excitotoxic lesions of the basal forebrain: a significant role for the cortical cholinergic system in attentional function. *J Neurosci* 14: 2313–2326, 1994.

Muir JL, Everitt BJ, Robbins TW. Reversal of visual attentional dysfunction following lesions of the cholinergic basal forebrain by physostigmine and nicotine but not by the 5-HT3 receptor antagonist, ondansetron. *Psychopharmacology (Berl)* 118: 82–92, 1995.

Nicolelis MA, Fanselow EE. Dynamic shifting in thalamocortical processing during different behavioural states. *Philos Trans R Soc Lond B Biol Sci* 357: 1753–1758, 2002.

Nunez A, Dominguez S, Buno W, Fernandez de Sevilla D. Cholinergic-mediated response enhancement in barrel cortex layer V pyramidal neurons. *J Neurophysiol* 108: 1656–1668, 2012.

Oken BS, Salinsky MC, Elsas SM. Vigilance, alertness, or sustained attention: physiological basis and measurement. *Clin Neurophysiol* 117: 1885–1901, 2006.

Pais-Vieira M, Lebedev MA, Wiest MC, Nicolelis MA. Simultaneous top-down modulation of the primary somatosensory cortex and thalamic nuclei during active tactile discrimination. *J Neurosci* 33: 4076–4093, 2013.

Pang K, Williams MJ, Egeth H, Olton DS. Nucleus basalis magnocellularis and attention: effects of muscimol infusions. *Behav Neurosci* 107: 1031–1038, 1993.

Pantoja J, Ribeiro S, Wiest M, Soares E, Gervasoni D, Lemos NA, Nicolelis MA. Neuronal activity in the primary somatosensory thalamocortical loop is modulated by reward contingency during tactile discrimination. *J Neurosci* 27: 10608–10620, 2007.

Paxinos G, Watson C. *The Rat Brain in Stereotaxic Coordinates*. Waltham, MA: Academic Press/Elsevier, 2007.

Pinto L, Goard MJ, Estandian D, Xu M, Kwan AC, Lee SH, Harrison TC, Feng G, Dan Y. Fast modulation of visual perception by basal forebrain cholinergic neurons. *Nat Neurosci* 16: 1857–1863, 2013.

Pleger B, Blankenburg F, Ruff CC, Driver J, Dolan RJ. Reward facilitates tactile judgments and modulates hemodynamic responses in human primary somatosensory cortex. *J Neurosci* 28: 8161–8168, 2008.

Rasmusson DD, Smith SA, Semba K. Inactivation of prefrontal cortex abolishes cortical acetylcholine release evoked by sensory or sensory pathway stimulation in the rat. *Neuroscience* 149: 232–241, 2007.

Richardson RT, DeLong MR. Context-dependent responses of primate nucleus basalis neurons in a go/no-go task. *J Neurosci* 10: 2528–2540, 1990.

Saper CB. Organization of cerebral cortical afferent systems in the rat. II. Magnocellular basal nucleus. *J Comp Neurol* 222: 313–342, 1984.

Sarter M, Hasselmo ME, Bruno JP, Givens B. Unraveling the attentional functions of cortical cholinergic inputs: interactions between signal-driven and cognitive modulation of signal detection. *Brain Res Brain Res Rev* 48: 98–111, 2005.

Steinmetz PN, Roy A, Fitzgerald PJ, Hsiao SS, Johnson KO, Niebur E. Attention modulates synchronized neuronal firing in primate somatosensory cortex. *Nature* 404: 187–190, 2000.

Szymusiak R. Magnocellular nuclei of the basal forebrain: substrates of sleep and arousal regulation. *Sleep* 18: 478–500, 1995.

Szymusiak R, Alam N, McGinty D. Discharge patterns of neurons in cholinergic regions of the basal forebrain during waking and sleep. *Behav Brain Res* 115: 171–182, 2000.

Tremblay N, Warren RA, Dykes RW. Electrophysiological studies of acetylcholine and the role of the basal forebrain in the somatosensory cortex of the cat. II. Cortical neurons excited by somatic stimuli. *J Neurophysiol* 64: 1212–1222, 1990.

Verdier D, Dykes RW. Long-term cholinergic enhancement of evoked potentials in rat hindlimb somatosensory cortex displays characteristics of long-term potentiation. *Exp Brain Res* 137: 71–82, 2001.

Voytko ML, Olton DS, Richardson RT, Gorman LK, Tobin JR, Price DL. Basal forebrain lesions in monkeys disrupt attention but not learning and memory. *J Neurosci* 14: 167–186, 1994.

Webster HH, Rasmusson DD, Dykes RW, Schliebs R, Schober W, Bruckner G, Biesold D. Long-term enhancement of evoked potentials in raccoon somatosensory cortex following co-activation of the nucleus basalis of Meynert complex and cutaneous receptors. *Brain Res* 545: 292–296, 1991.

Weinberger NM. The nucleus basalis and memory codes: auditory cortical plasticity and the induction of specific, associative behavioral memory. *Neurobiol Learn Mem* 80: 268–284, 2003.

Wiest M, Thomson E, Meloy J. Multielectrode recordings in the somatosensory system. *Methods for Neural Ensemble Recordings*, edited by Nicolelis MAL. Boca Raton, FL: CRC, 2008.

Wiest MC, Bentley N, Nicolelis MA. Heterogeneous integration of bilateral whisker signals by neurons in primary somatosensory cortex of awake rats. *J Neurophysiol* 93: 2966–2973, 2005.

Wiest MC, Thomson E, Pantoja J, Nicolelis MA. Changes in S1 neural responses during tactile discrimination learning. *J Neurophysiol* 104: 300–312, 2010.

Wilson FA, Rolls ET. Learning and memory is reflected in the responses of reinforcement-related neurons in the primate basal forebrain. *J Neurosci* 10: 1254–1267, 1990.

Yu AJ, Dayan P. Uncertainty, neuromodulation, and attention. *Neuron* 46: 681–692, 2005.

Zaborszky L, Csordas A, Mosca K, Kim J, Gielow MR, Vadasz C, Nadasdy Z. Neurons in the basal forebrain project to the cortex in a complex topographic organization that reflects corticocortical connectivity patterns: an experimental study based on retrograde tracing and 3D reconstruction. *Cereb Cortex*. First published August 19, 2013; doi:10.1093/cercor/bht210.

Zaborsky L, van den Pol A, Gyengesi E. The basal forebrain cholinergic projection system in mice. *The Mouse Nervous System*, edited by Paxinos G, Watson C, Puelles L. Amsterdam: Elsevier Academic: 2012, p. 684–718.

Zar JH. *Biostatistical Analysis*. Upper Saddle River, NJ: Prentice Hall, 1996.

Zhang H. Exploring conditions for the optimality of naive Bayes. *Int J Pattern Recogn* 19: 183–198, 2005.